Prostaglandin E_2 2 Signaling and Bacterial Infection Recruit Tumor-Promoting Macrophages to Mouse Gastric Tumors

HIROKO OSHIMA,* KYOJI HIOKI,‡ BORYANA K. POPIVANOVA,* KEISUKE OGUMA,* NICO VAN ROOIJEN,§ TOMO–O ISHIKAWA,* and MASANOBU OSHIMA*

*Division of Genetics, Cancer Research Institute, Kanazawa University, Kanazawa; ‡Gnotobiology Laboratory, Central Institute for Experimental Animals, CIEA, Kawasaki, Japan; and §Department of Molecular Cell Biology, Vrije Universiteit, Amsterdam, The Netherlands

BACKGROUND & AIMS: *Helicobacter pylori* infection induces an inflammatory response, which can contribute to gastric tumorigenesis. Induction of cyclooxygenase-2 (COX-2) results in production of prostaglandin E_2 (PGE_2), which mediates inflammation. We investigated the roles of bacterial infection and PGE_2 signaling in gastric tumorigenesis in mice. **METHODS:** We generated a germfree (GF) colony of *K19-Wnt1/C2mE* mice (*Gan* mice); these mice develop gastric cancer. We examined tumor phenotypes, expression of cytokines and chemokines, and recruitment of macrophages. We also investigated PGE_2 signaling through the PGE_2 receptor subtype 4 (EP4) in *Gan* mice given specific inhibitors. **RESULTS:** *Gan* mice raised in a specific pathogen-free facility developed large gastric tumors, whereas gastric tumorigenesis was significantly suppressed in GF-*Gan* mice; reconstitution of commensal flora or infection with *Helicobacter felis* induced gastric tumor development in these mice. Macrophage infiltration was significantly suppressed in the stomachs of GF-*Gan* mice. *Gan* mice given an EP4 inhibitor had decreased expression of cytokines and chemokines. PGE_2 signaling and bacterial infection or stimulation with lipopolysaccharide induced expression of the chemokine C-C motif ligand 2 (CCL2) (which attracts macrophage) in tumor stromal cells or cultured macrophages, respectively. CCL2 inhibition suppressed macrophage infiltration in tumors, and depletion of macrophages from the tumors of *Gan* mice led to signs of tumor regression. Wnt signaling was suppressed in the tumors of GF-*Gan* and *Gan* mice given injections of tumor necrosis factor-α neutralizing antibody. **CONCLUSIONS: Bacterial infection and PGE_2 signaling are required for gastric tumorigenesis in mice; they cooperate to up-regulate CCL2, which recruits macrophage to gastric tumors. Macrophage-derived tumor necrosis factor-α promotes Wnt signaling in epithelial cells, which contributes to gastric tumorigenesis.**

Keywords: Stomach Cancer; Tumor Promotion; Bacterial Infection.

BASIC–ALIMENTARY TRACT

Gastric cancer is the second most common cause of cancer-related death in the world, and *Helicobacter pylori* infection is closely associated with gastric cancer development.[1] Infections are estimated to be related to 15% of malignant cancer development, and infection-associated inflammation is a critical component of cancer development.[2] For example, an inflammatory response promotes tumor cell proliferation, metastasis, and survival, whereas it suppresses antitumor immune responses.[2–4] Moreover, the genetic polymorphisms in genes encoding inflammatory cytokines influence gastric tumorigenesis.[5] These results suggest that an inflammatory cytokine network induced by *H pylori* infection plays a key role in gastric tumorigenesis.

Cycooxygenase-2 (COX-2) is an inducible enzyme for prostaglandin biosynthesis, which plays an important role in both inflammation and tumorigenesis.[6,7] Mouse model studies have indicated that induction of the COX-2/prostaglandin E_2 (PGE_2) pathway accelerates intestinal tumorigenesis through the induction of angiogenesis and suppression of apoptosis.[8,9] Among 4 PGE_2 receptors (EP1–EP4), EP4 receptor signaling has been shown to play an important role in intestinal tumorigenesis through the activation of epidermal growth factor receptor.[10] The expression of COX-2 is also found in more than 70% of gastric cancers,[11] which is suppressed by the eradication of *H pylori*,[12] suggesting COX-2 induction by infection in the gastric mucosa. Transgenic mice expressing COX-2 and a PGE_2 converting enzyme, microsomal prostaglandin E synthase-1 (mPGES-1), in the stomach develop hyperplasia with macrophage infiltration, indicating the role of PGE_2 in macrophage recruitment.[13] Tumor-associated macrophages (TAMs) play an important role in tumorigenesis through the enhancement of angiogenesis, migration, and remodeling.[14] Moreover, the simultaneous activation of Wnt and the PGE_2 pathways in the mouse stomach causes dysplastic tumor de-

Abbreviations used in this paper: COX-2, cyclooxygenase-2; *Gan*, Gastric neoplasia; GF, germfree; IL-1β, interleukin-1β; IL-6, interleukin-6; LPS, lipopolysaccharide; mPGES-1, microsomal prostaglandin E synthase-1; NF-κB, nuclear factor-κB; PGE_2, prostaglandin E_2; RT-PCR, reverse transcription-polymerase chain reaction; SPF, specific pathogen free; TAM, tumor-associated macrophage; TNF-α, tumor necrosis factor-α.

0016-5085/$36.00
doi:10.1053/j.gastro.2010.11.007

velopment.[15] Accordingly, it is possible that PGE_2-dependent macrophage recruitment is one of the important mechanisms underlying the *H pylori* infection-associated inflammation in gastric tumorigenesis. However, the relationship between bacterial infection and PGE_2 signaling in gastric tumorigenesis remains unclear.

Commensal bacteria constitutively stimulate the intestinal mucosa, inducing cytokines and chemokines at a basal level, which is important for homeostasis of the intestinal mucosa.[16] The present study shows that indigenous bacteria constitutively stimulate the gastric mucosa, which is required for tumorigenesis in the Wnt-activated and PGE_2-induced gastric mucosa. Bacterial colonization and PGE_2 signaling through EP4 receptor cooperatively induced the expression of CCL2, which was a major pathway for macrophage recruitment in the gastric mucosa. Furthermore, depletion of macrophages caused regressive signs of tumors. These results indicate that bacterial infection and PGE_2 signaling cooperatively recruit macrophages to the gastric mucosa, which promotes gastric cancer development.

Materials and Methods

Animal Experiments

The construction of *K19-Wnt1* [*Tg(Krt19-Wnt1) 2Maos*], *K19-C2mE* [*Tg(Krt19-Ptgs2,Krt19-Ptges)8Tko*], and *K19-Wnt1/C2mE* (*Gan* for Gastric neoplasia) [*Tg(Krt19-Wnt1)2Maos/Tg(Krt19-Ptgs2,Krt19-Ptges)8Tko*] transgenic mice was described previously (Supplementary Table 1).[13,15] All mice used in the present study were backcrossed to C57BL/6 mice more than 12 times. Germfree (GF) mouse colonies of all genotypes and wild-type mice were established by cesarean derivation at the Central Institute for Experimental Animals (CIEA, Kawasaki, Japan), and the mice were raised in GF isolators under GF conditions. During the experiments, GF conditions were monitored by cultures of feces, bedding, and swabs in thioglycollate medium or potato dextrose broth every 2–5 weeks (Supplementary Table 2). Specific pathogen free (SPF)-raised mice were maintained in the SPF facility at Kanazawa University. The excluded pathogens in the SPF facility are listed in Supplementary Table 3. Mice were killed and examined at 30 and 55 weeks of age (n = 4–6 mice), and all experimental groups consisted of both female and male mice. Half of the glandular stomach was used for the histologic analysis, and the other half was used for RNA and protein sample preparation. Six GF *Gan* mice were moved to the SPF facility at 7 weeks of age, reconstituted with commensal flora by cohousing with SPF mice and adding dirty bedding from other cages and examined at 30 weeks of age. *Helicobacter felis* (ATCC 49179) were inoculated at 10^8/mouse PO to GF *Gan* mice at 30 weeks of age (n = 3 mice), and gastric phenotypes were examined at 55 weeks of age. The time course and experimental conditions for each group are shown in Supplementary Figure 1. All animal experiments were carried out according to the protocol approved by the Committee on Animal Experimentation of Kanazawa University.

Gastric pH Measurement

Gastric pH was measured as described.[17] Briefly, mice were fasted overnight before necropsy. Sterile water (1.5 mL) was injected into the stomach, the stomach was massaged gently, and the pH of the gastric contents was measured using a pH meter.

Drug Treatment Experiments

The EP4 receptor inhibitor RQ-00015986/CJ-42794[18] was provided from RaQualia Pharma Inc (Taketoyo, Japan). *Gan* mice were treated with RQ-00015986 at 100 mg/kg/day PO from 27 or 52 weeks of age for 3 weeks (n = 4 or 5 mice). For inhibition of tumor necrosis factor (TNF)-α or CCL2, *Gan* mice were injected with a neutralizing antibody against TNF-α (AB-410-NA; R&D Systems, Minneapolis, MN) at 8 mg/kg/day intraperitoneally for 6 days (n = 3 mice) or an antibody against CCL2 (AF-479-NA; R&D Systems) at 1 mg/kg/day intraperitoneally for 3 days (n = 3 mice), respectively. Macrophages were depleted in vivo by injection of 200 μL clodronate (dichloromethylene bisphosphonate)-loaded liposomes intravenously every 3 days for 2 weeks as previously described.[19] Clodronate was a gift from Roche Diagnostics GmbH (Mannheim, Germany) and was encapsulated in liposomes as described previously.[20]

Histology and Immunohistochemistry

Stomach tissues were fixed in 4% paraformaldehyde, paraffin embedded, and sectioned at 4-μm thickness. These sections were stained with H&E or processed for immunostaining. Tissues were also embedded in OCT compound (Sakura Finetechnical, Tokyo, Japan), frozen in liquid nitrogen, and sectioned at 10-μm thickness. The frozen sections were used for CCL2 immunostaining. Antibodies against the proton pump (MBL, Nagoya, Japan), F4/80 (Serotec, Oxford, UK), β-catenin (Sigma, St. Louis, MO), CCL2 (Hycult Biotech, Uden, The Netherlands), EP4 (MBL), CD44 (Millipore, Billerica, MA), EphB3 (Bioworld Technology, St. Louis Park, MN), and Ki-67 (Dako, Carpinteria, CA) were used as the primary antibodies. Staining signals were visualized using the Vectastain Elite Kit (Vector Laboratories, Burlingame, CA). For fluorescence immunostaining, Alexa Fluor 594 or Alexa Fluor 488 antibody (Molecular Probes, Eugene, OR) was used as the secondary antibody. Apoptosis was examined using the ApopTag Apoptosis Detection Kit (Millipore). The mean index for F4/80 (macrophage), proton pump (parietal cell), Ki-67, or apoptosis was calculated by counting labeled cells per microscopic field (200×) in 5 fields.

Scoring Tumor Volume and Preneoplastic Lesions

The mucosal thickness (tumor height) of the gastric tumors of *Gan* mice and the normal stomach of wild-type mice was measured from histology sections. The mucosal thickness relative to that of wild-type mice was calculated. The number of preneoplastic lesions in the whole glandular stomach of *K19-Wnt1* mice was counted under a dissection microscope after staining with 0.05% toluidine blue. The histologic characteristics of gastric tumors and preneoplastic lesions were described previously.[15] The histology of these lesions was confirmed after scoring.

Cell Culture Experiments

The RAW264 macrophage cells (RIKEN BioResource Center, Tsukuba, Japan) were treated with lipopolysaccharide (LPS) (Sigma) for 24 hours at 1, 10, 50, 100, 1000, or 10,000 pg/mL with or without treatment with a COX-2 inhibitor, celecoxib, or RQ00015986 at 10 μmol/L, and the expression levels of CCL2 and cytokines were examined. Celecoxib was provided by Pfizer (New York, NY). For the primary culture of gastric epithelial cells, the glandular stomach of *K19-Wnt1* mice was treated with 0.1% collagenase followed by trypsin, and epithelial cells were cultured in matrigel (BD Pharmingen, Franklin Lakes, NJ) with epidermal growth factor (EGF) (−) primary culture medium.[13] The primary cultured cells were treated with RQ00015986 at 10 μmol/L for 6 days, and organoid structures consisting of epithelial cells larger than 0.2 mm in diameter were counted.

Immunoblotting Analysis

The tissues were homogenized and sonicated in lysis buffer. Thereafter, the specimens were centrifuged at 20,000*g*, and 10 μg of the supernatant protein sample was separated in a 10% sodium dodecyl sulfate-polyacrylamide gel. An antibody against unphosphorylated active β-catenin (Millipore) was used as the primary antibody. Anti-β-actin (Sigma) was used as the internal control. The ECL detection system (GE Healthcare, Buckinghamshire, UK) was used to detect the signals.

Real-Time Reverse-Transcription Polymerase Chain Reaction

Tumor stroma and epithelial cell samples were separately collected from frozen sections using Laser Microdissection (Leica, Wetzlar, Germany). Total RNA was extracted from the tissues or microdissected samples using ISOGEN (Nippon Gene, Tokyo, Japan), reverse transcribed with PrimeScript RT reagent Kit (Takara, Tokyo, Japan), and polymerase chain reaction (PCR) amplified by Stratagene Mx300P (Agilent Technologies, Santa Clara, CA) using SYBR Premix ExTaqII (Takara). Primers for the real-time reverse-transcription polymerase chain reaction (RT-PCR) were purchased (Takara), and the primer sequences are shown in Supplementary Table 4.

Statistical Analysis

The data were analyzed using the unpaired *t* test and are presented as the means ± standard deviation. A value of $P < .05$ was considered to be statistically significant.

Results

Constitutive Stimulation of Gastric Mucosa by Indigenous Bacteria

To determine whether indigenous bacteria in the stomach stimulate the gastric mucosa, we examined the expression of cytokines and chemokines in the glandular stomach of germfree (GF) wild-type mice and control SPF mice by real-time RT-PCR (Figure 1*A*). Importantly, the expression levels of TNF-α, interleukin (IL)-1β, keratinocyte-derived chemokine (KC), and macrophage inflammatory protein-2 (MIP-2) decreased significantly in the GF mouse stomach compared with the SPF mice, whereas IL-6 expression slightly increased. These results indicate that commensal bacteria constitutively stimulate the gastric mucosa to induce inflammatory cytokines and chemokines at a basal level.

Gan mice were previously constructed by crossing *K19-Wnt1* and *K19-C2mE* mice (Supplementary Table 1).[13,15] We examined the number of parietal cells by immunostaining and measured intragastric pH in these models because bacterial growth is affected by intragastric acidity. The mean parietal cell index was similar in all strains, and the intragastric pH was around 3.5 (Figure 1*B–D*). However, in the dysplastic tumors of *Gan* mice, the number of parietal cells decreased significantly, and intragastric pH increased at 50–55 weeks of age. These results indicate that gastric acidity is not changed in *Gan* mice at early stages of disease compared with other models until large tumors develop at the later stages.

Suppression of Gastric Tumorigenesis in GF Mice

Gan mice raised in an SPF facility (SPF-*Gan*) developed large gastric tumors by 55 weeks of age (Figure 2*A* and *B*), and the mean tumor height increased to approximately 1.5-fold when compared with that at 30 weeks of age. In contrast, gastric tumorigenesis was significantly suppressed in the GF *Gan* (GF-*Gan*) mice, and the mean mucosal thickness of GF-*Gan* mice was less than 40% of the age-matched SPF-*Gan* mice (Figure 2*A* and *B*, Supplementary Figure 2). Approximately 40% of the SPF-*Gan* mice showed a moribund phenotype and thus were killed by 60 weeks of age, whereas all GF-*Gan* mice survived by 55 weeks of age (Figure 2*C*). Importantly, reconstitution of commensal bacteria in GF-*Gan* mice resulted in development of gastric tumors that were significantly larger than those of GF-*Gan* mice (Figure 2*A*, Supplementary Figure 2), and treatment of SPF-*Gan* mice with antibiotics significantly suppressed gastric tu-

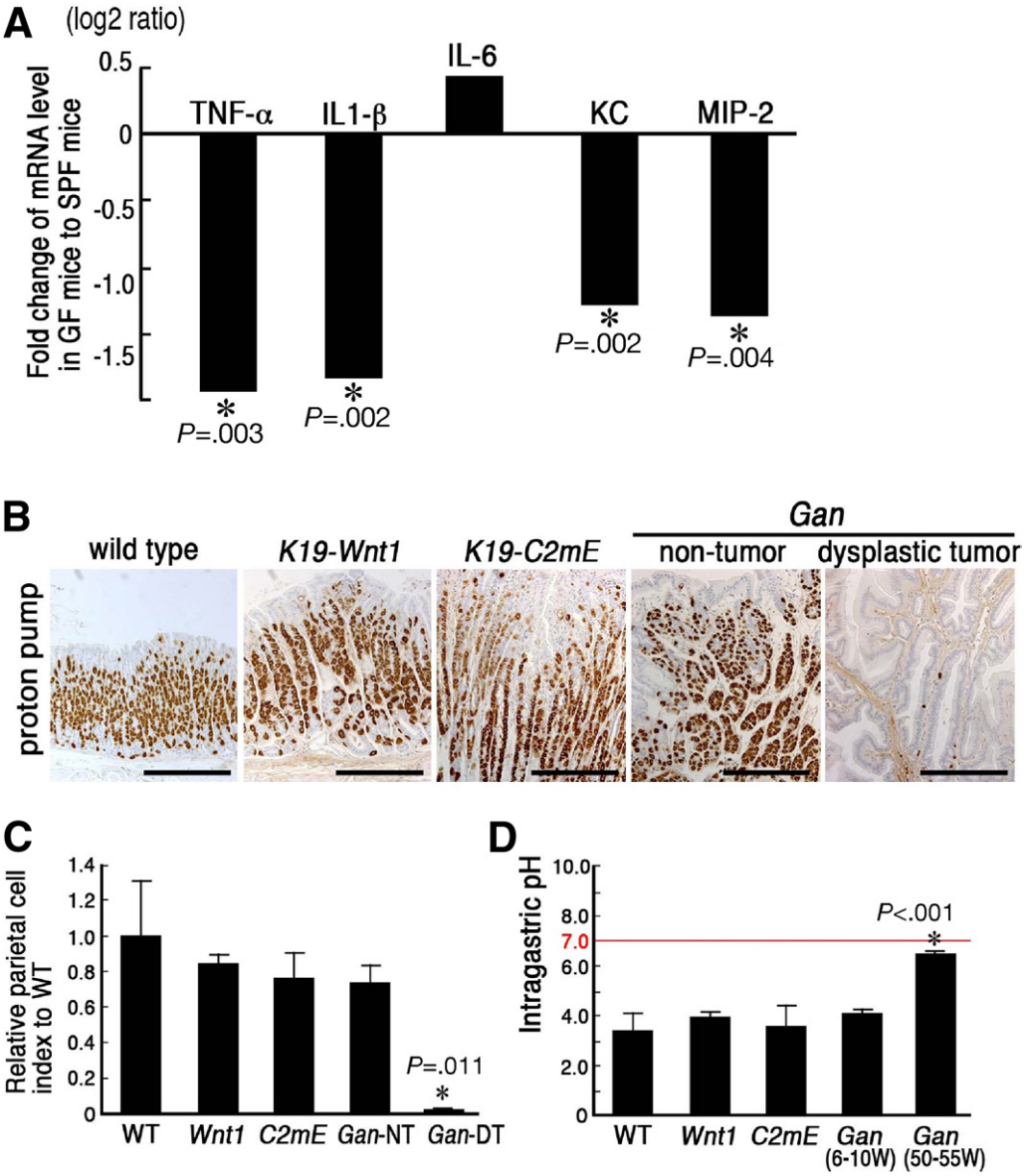

Figure 1. Stimulation of normal gastric mucosa by indigenous bacteria. (*A*) Messenger RNA (mRNA) levels of cytokines and chemokines in the gastric mucosa of the germfree (GF)-wild-type mice (mean log2 ratio to the SPF mouse level). *$P < .05$. (*B*) Immunostaining for proton pumps (parietal cells) in the gastric mucosa of the indicated strains. *Scale bars*, 100 μm. (*C*) The parietal cell index relative to the wild-type mouse level (mean ± standard deviation [SD]). *$P < .05$ vs the wild-type level (*WT*). *Gan*-NT, *Gan* nontumor; *Gan*-DT, *Gan* dysplastic tumor. (*D*) Intragastric pH of the indicated mouse strains (mean ± SD). *$P < .001$ vs the wild-type level (*WT*).

mor growth (Supplementary Figure 3). These results indicate that colonization of indigenous bacteria is required for gastric tumor development.

Moreover, infection with *Helicobacter felis*, separate species of *Helicobacter pylori*, in the GF-*Gan* mouse stomach at 30 weeks of age (GF->*H felis* mice) induced the development of gastric tumors by 55 weeks of age (Figure 2*A* and *B*). The infection of *H felis* in gastric glands was confirmed by microscopy of histology sections (Supplementary Figure 4). These results also indicate the role of infection in gastric tumorigenesis.

Apoptotic cells were found only on the mucosal surface of gastric tumors (Figure 2*D*), and the mean apoptosis index was 42.4% and 40.0% on the mucosal surface in SPF-*Gan* and GF-*Gan* mice, respectively. On the other hand, the number of Ki-67-labeled proliferating cells was significantly lower in the GF-*Gan* mouse stomach (Figure 2*E* and *F*), suggesting that bacterial colonization contributes to the tumor cell proliferation.

Suppression of Gastric Tumorigenesis by Inhibition of the PGE$_2$ Receptor EP4

There are 4 PGE$_2$ receptors (EP1—EP4), and the expression level of EP4 was increased significantly in *Gan* mouse tumors.[21] SPF-*Gan* mice were thus treated with a specific EP4 inhibitor, RQ-00015986, for 3 weeks from 52

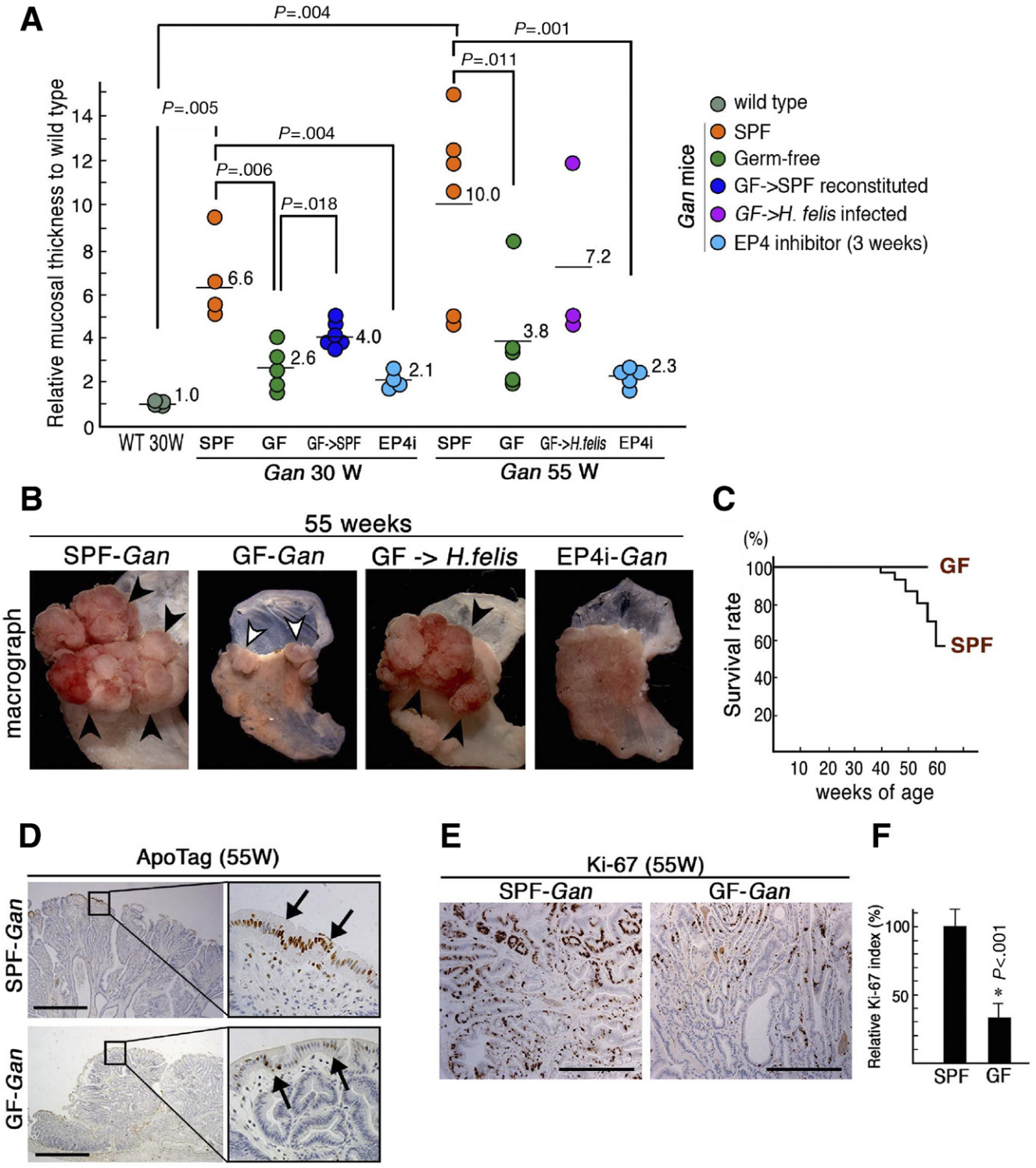

Figure 2. Suppression of gastric tumorigenesis in germfree (*GF*) *Gan* mice. (*A*) The gastric mucosal thickness (tumor height) of SPF-*Gan* (*SPF*), GF-*Gan* (*GF*), commensal flora-reconstituted GF-*Gan* (*GF->SPF*), *H felis*-infected GF-*Gan* (*GF->H felis*), and EP4 inhibitor-treated-*Gan* (*EP4i*) mice at 30 and 55 weeks of age relative to wild-type mice (*WT*). (*B*) Representative macroscopic photographs of the stomach of the indicated group of *Gan* mice at 55 weeks of age. *Black arrowheads* indicate tumors, whereas the *white arrowheads* indicate suppressed tumorous lesions in the *GF*-Gan mouse. (*C*) The survival rate of the SPF-*Gan* and GF-*Gan* mice. All GF-*Gan* mice were used for experiments at 55 weeks of age. (*D*) Apoptosis analyses of SPF-*Gan* and GF-*Gan* mouse gastric tumors. *Arrows* indicate apoptotic cells on the mucosal surface of tumors. (*E*) Ki-67 immunostaining in the gastric tumors of SPF-*Gan* and GF-*Gan* mice. *Scale bars* in *D* and *E*, 100 μm. (*F*) Relative mean Ki-67 labeling index (mean ± standard deviation). *$P < .001$ vs SPF level.

weeks of age (Supplementary Figure 1). Notably, gastric tumors regressed significantly following inhibition of EP4, and the mean tumor size decreased to 23% of that of the age-matched SPF-*Gan* mice (Figure 2*A* and *B*). Moreover, treatment of SPF-*Gan* mice with an EP4 inhibitor during the early stage of tumorigenesis from 27 weeks of age also suppressed tumor development significantly. These results indicate that EP4 signaling plays an important role in gastric tumorigenesis.

Bacterial Infection and EP4 Signaling for Inflammatory Responses

Submucosal lymphocyte infiltration was found in the SPF-*Gan* and GF->*H felis* mouse tumors but not in GF-*Gan* and EP4 inhibitor-treated *Gan* (EP4i-*Gan*) mice (Figure 3*A*), suggesting that both bacterial infection or colonization and EP4 signaling are required for inflammatory responses. Moreover, the expression level of proinflammatory cytokines, TNF-α, IL-1β, and IL-6 and chemokines, KC and MIP-2, were significantly elevated in the SPF-*Gan* and GF->*H felis* gastric tumors (Figure 3*B*), indicating inflammatory responses in the stomachs of these mice. In contrast, the expression of these cytokines and chemokines was not induced in the GF-*Gan* and EP4i-*Gan* mouse stomachs. The transgenic expression of COX-2 (*Ptgs2*) in the stomach was confirmed in all mouse groups except the wild-type mice, indicating that the PGE$_2$ level was elevated in all groups of *Gan* mice. These results indicate that both infection and EP4 signaling are required for inflammatory responses in the stomach.

The expression of proinflammatory cytokines was predominantly detected in stromal cells when compared with tumor epithelial cells in SPF-*Gan* tumors (Figure 3*C*), suggesting that stromal macrophages were the major source of these cytokines. We thus examined macrophage infiltration by immunostaining. As expected, numerous macrophages were found in the SPF-*Gan* and GF->*H felis* *Gan* mouse tumors, whereas macrophage infiltration was suppressed in the GF-*Gan* and EP4i-*Gan* mice (Figure 3*D*). The number of macrophages in the GF-*Gan* and EP4i-*Gan* mouse stomachs decreased significantly to 11% and 33% of the SPF-*Gan* mouse level, respectively (Figure 3*E*). These results suggest that cooperation of bacterial infection or colonization with EP4 signaling contributes to macrophage recruitment to the gastric mucosa.

To examine the role of macrophages in gastric tumorigenesis, SPF-*Gan* mice were treated with clodronate liposomes to deplete macrophages in vivo. Macrophage-depleted areas were found by immunostaining in the clodronate liposome-injected *Gan* mouse tumors (Figure 3*F*). In the macrophage-depleted area, tumors showed regressive signs with atrophic changes of tumor cells or peel-off of tumor epithelial cells from the mucosal surface, suggesting that macrophages are important for the maintenance or survival of tumor epithelial cells.

Induction of CCL2 by Bacterial Infection and EP4 Signaling

The expression level of macrophage-tropic chemokines was examined in the SPF-*K19-C2mE* and GF-*K19-C2mE* mouse stomach. The PGE$_2$ pathway but not Wnt signaling is activated in the glandular stomach of *K19-C2mE* mice (Supplementary Table 1). Importantly, expression of CCL2 and CCL8 increased significantly in the SPF-*K19-C2mE* mouse stomach compared with that in the wild-type mice (Figure 4*A*). In contrast, expression of CCL2 and CCL8 was not induced in the GF-*K19-C2mE* mouse stomach. Induction of CCL2 and CCL8 expression was also found in gastric tumors of SPF-*Gan* mice but not in GF-*Gan* mice (Figure 4*B*). These results suggest that PGE$_2$ signaling and bacterial colonization cooperatively induce expression of CCL2 and CCL8 in the gastric mucosa.

Because CCL2 is an important chemokine for macrophage infiltration in colon tumors,[22] we further examined CCL2 expression. CCL2-expressing cells were detected by immunostaining in the stroma of SPF-*Gan* mouse tumors where macrophages were accumulated (Figure 4*C*), suggesting that macrophages express CCL2. The stimulation of RAW264 macrophage cells with LPS induced the expression of CCL2 in a dose-dependent manner (Figure 4*D*). A low concentration of LPS was used for further experiments to examine the effect of low counts of indigenous bacterial colonization in the stomach. Importantly, treatment of RAW264 macrophages with an EP4 inhibitor significantly suppressed LPS-induced CCL2 expression (Figure 4*E*), suggesting that both EP4 signaling and LPS stimulation are required for CCL2 induction in macrophages.

To examine the role of CCL2 in macrophage recruitment in gastric tumors, SPF-*Gan* mice were treated with an anti-CCL2 neutralizing antibody. Notably, inhibition of CCL2 suppressed macrophage infiltration in tumors, although a few macrophages were still detected (Figure 4*F*), suggesting that CCL2 is a major chemokine that recruits macrophages to gastric tumors. In the macrophage-depleted tumor areas caused by CCL2 inhibition, tumors showed regressive signs, which was similar to the observations in the clodronate liposome-treated *Gan* mice (Figure 3*F*).

M2 Type Polarization of Macrophages in Gastric Tumors

TAMs play a pivotal role in tumor development.[14] Macrophage activation is classified as "classically" activated (M1) or "alternatively" activated (M2) type, and TAMs generally express characteristics of M2-polarized macrophages.[23] Interestingly, the expression of M2 macrophage markers, Ym1, Ym2, arginase 1 (Arg1), and transforming growth factor-β, increased significantly in both the SPF-*K19-C2mE* stomach and SPF-*Gan* tumors (Supplementary Figure 5*A*). Consistently, expression of

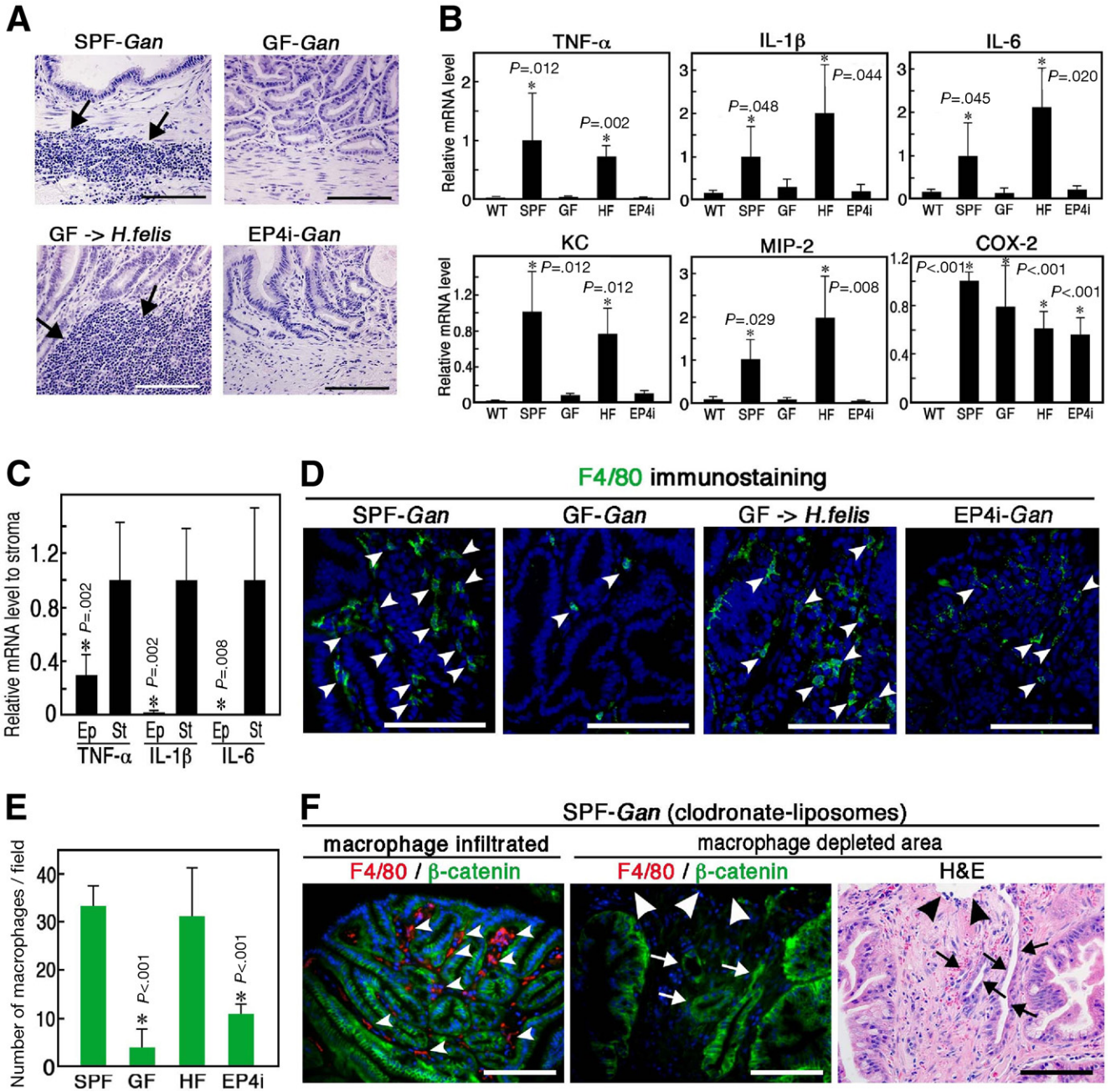

Figure 3. Macrophage recruitment in the *Gan* mouse tumors. (*A*) H&E staining of the SPF-*Gan*, GF-*Gan*, *H felis*-infected GF-*Gan* (GF->*H felis*), and EP4 inhibitor-treated *Gan* (EP4i-*Gan*) mouse stomachs. *Arrows* indicate lymphocyte infiltration. *Scale bars*, 100 μm. (*B*) Relative messenger RNA (mRNA) levels of inflammatory cytokines, chemokines, and COX-2 in wild-type mouse stomach (*WT*) and SPF-*Gan* (*SPF*), GF-*Gan* (*GF*), *H felis*-infected GF-*Gan* (*HF*), and EP4i-*Gan* (*EP4i*) mouse gastric tumors (mean ± standard deviation [SD]). *$P < .05$ vs wild-type level. (*C*) The mRNA level of inflammatory cytokines in the microdissected tumor epithelial cells (*Ep*) relative to the level in the tumor stroma (*St*). *$P < .01$. (*D*) Immunostaining of F4/80 (*green*) with 4',6-diamidino-2-phenylindole staining (*blue*) in gastric tumors of the indicated groups. *Arrowheads* indicate F4/80-positive macrophages. *Scale bars*, 100 μm. (*E*) The mean number of F4/80-positive macrophages per microscopic field (mean ± SD). *$P < .001$ vs SPF level. (*F*) Immunostaining of F4/80 (*red*) and β-catenin (*green*) in gastric tumors of a control *Gan* mouse (*left*) and clodronate liposome-treated *Gan* mouse (*center*). H&E staining of serial section of a clodronate liposome-treated *Gan* mouse tumor (*right*). *Scale bars*, 100 μm. *Arrowheads* (*left*) indicate macrophages. *Arrowheads* and *arrows* (*center* and *right*) indicate the mucosal surface of the tumor and tumor cells, respectively, in the macrophage-depleted area.

an M2 marker, mannose receptor, was detected by immunohistochemistry in the SPF-*Gan* mouse tumors (Supplementary Figure 5*B*). It has been reported that $CD4^+$ T cells regulate the M2 properties of macrophages.[24] CD4+ T cells infiltrated into the SPF-*Gan* mouse tumors (Supplementary Figure 5*C*). However, M2 macrophages were also found in SPF-*Rag2*$^{-/-}$ *K19-C2mE* mouse stomachs (Supplementary Figure 5*D*), suggesting

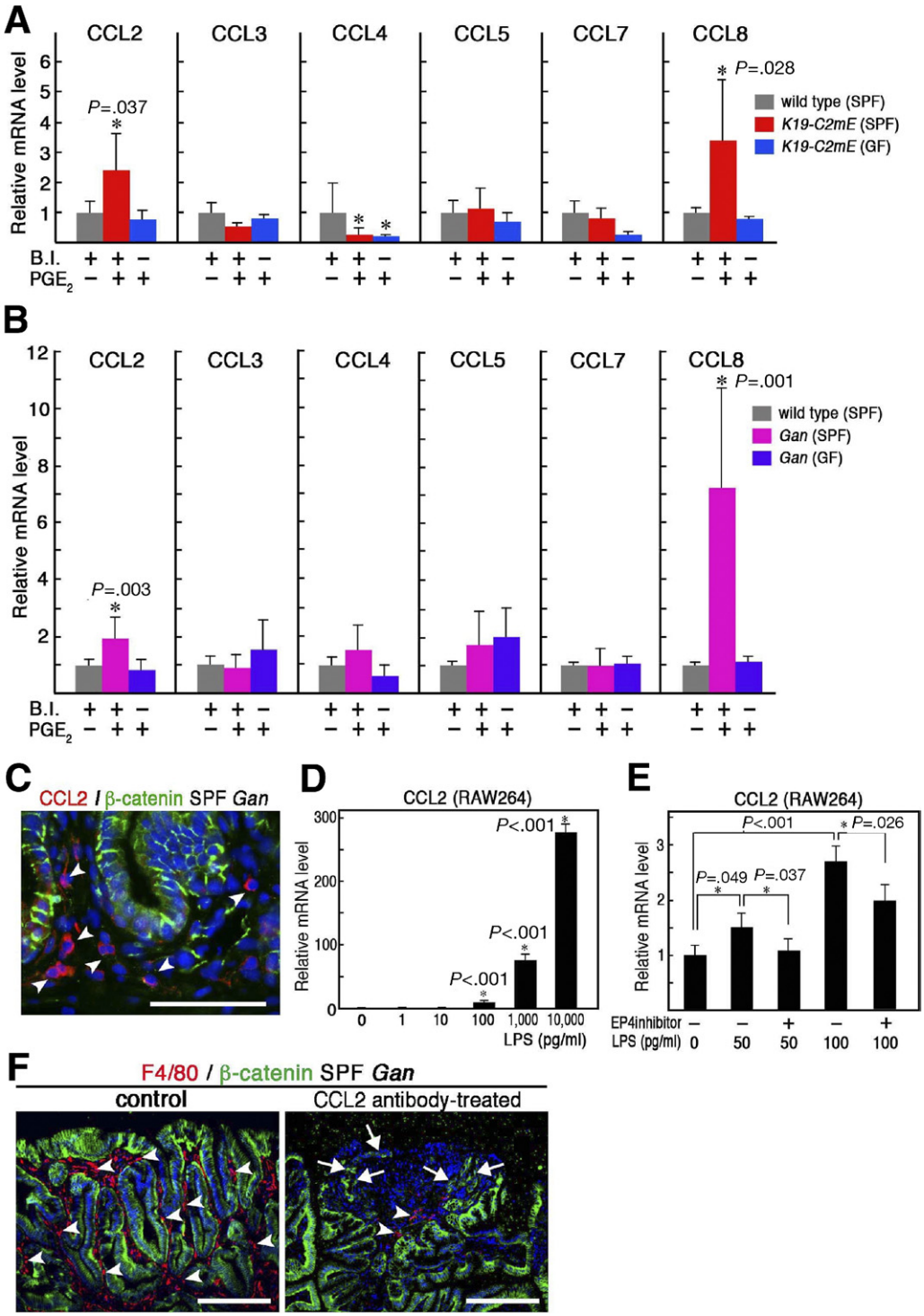

Figure 4. Chemokine induction by bacterial colonization and PGE$_2$ signaling. (*A* and *B*) The messenger RNA (mRNA) levels of the indicated chemokines in SPF-*K19-C2mE* (*red*) and GF-*K19-C2mE* (*blue*) gastric mucosa (*A*) and SPF-*Gan* (*pink*) and GF-*Gan* (*purple*) gastric tumors (*B*) relative to that in the control SPF wild-type mouse stomach (*gray*) (mean ± standard deviation [SD]). The indigenous bacterial colonization (*B.I.*) and PGE$_2$ transgenic status (*PGE$_2$*) are indicated at the bottom. *$P < .05$ vs wild-type level. (*C*) Immunostaining of CCL2 (*red*, *arrowheads*) and β-catenin (*green*) with 4',6-diamidino-2-phenylindole (DAPI) staining (*blue*) in SPF-*Gan* gastric tumor. *Scale bar*, 100 μm. (*D*) The mRNA levels of CCL2 in the LPS-stimulated RAW264 cells relative to that in the unstimulated control cells (mean ± SD). *$P < .001$ vs control level. (*E*) The mRNA levels of CCL2 in RAW264 cells with indicated treatment relative to the level in the unstimulated RAW264 cells (mean ± SD). *$P < .05$. (*F*) Immunostaining for F4/80 (*red*, *arrowheads*) and β-catenin (*green*) with DAPI staining (*blue*) in tumors of control SPF-*Gan* (*left*) and CCL2 antibody-treated SPF-*Gan* mice (*right*). *Scale bars*, 100 μm. *Arrows* in *right panel* indicate regressed tumors in the macrophage-depleted area.

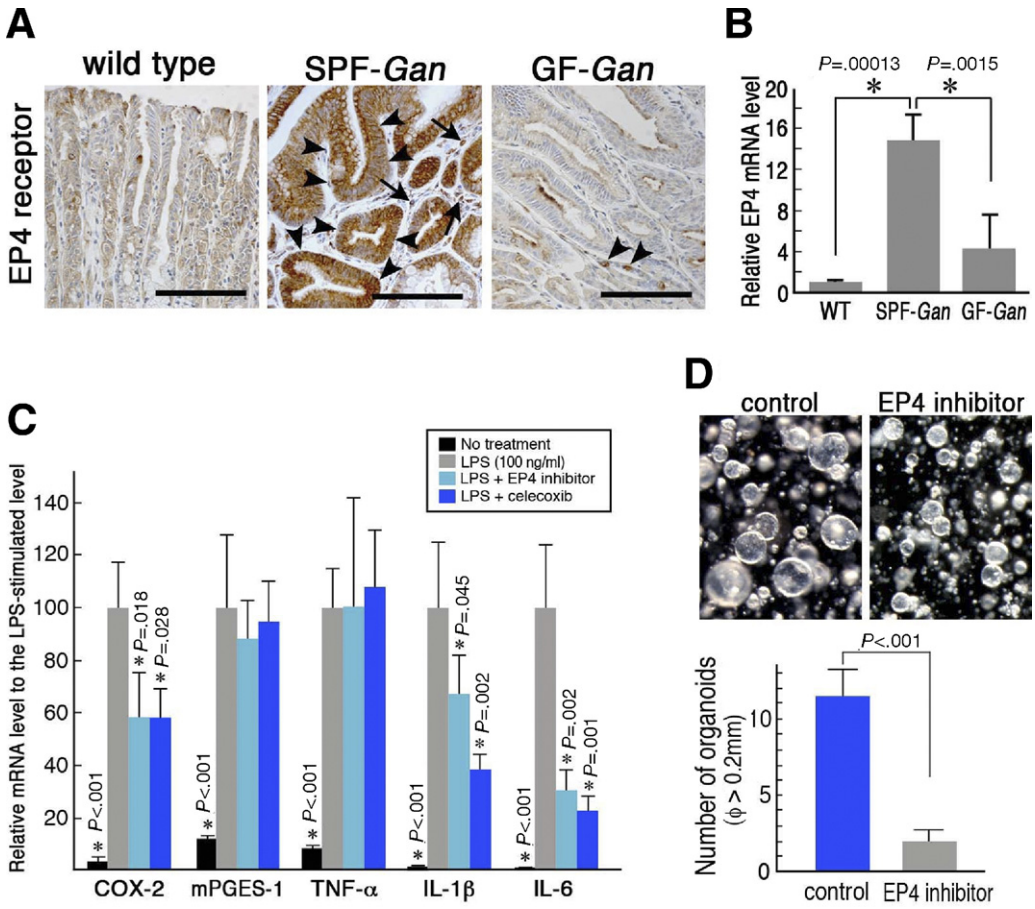

Figure 5. EP4 signaling on macrophages and epithelial cells. (*A*) Immunostaining of EP4 in the normal gastric mucosa of wild-type mouse and gastric tumors of SPF- and GF-*Gan* mice. *Arrowheads* and *arrows* indicate EP4 expression in the tumor epithelia and tumor stromal cells, respectively. *Scale bars*, 100 μm. (*B*) The messenger RNA (mRNA) levels of EP4 in gastric tumors of SPF-*Gan* and GF-*Gan* mice relative to the wild-type mouse level (mean ± standard deviation [SD]). *$P < .01$. (*C*) The mRNA levels of inflammatory cytokines in the control or drug-treated RAW264 cells relative to the level of LPS-stimulated RAW264 cells (mean ± SD). *$P < .05$ to the LPS-stimulated level. (*D*) Representative photographs of organoid structures formed by the primary cultured gastric epithelial cells in matrigel with EP4 inhibitor treatment (*top right*) and no-treatment control (*top left*). The mean number of organoids larger than 0.2 mm in diameter in the microscopic field on day 6 of culture (*bottom*) (mean ± SD). *$P < .001$.

that macrophages in the PGE_2-induced inflammation can be polarized to the M2 type in the absence of T cells.

EP4 Signaling on Macrophages and Epithelial Cells

Expression of the EP4 receptor was detected by immunostaining in both tumor epithelial cells and stromal cells of SPF-*Gan* mice, whereas it was rarely detected in the GF-*Gan* or wild-type mouse stomach (Figure 5*A*). Induction of EP4 in SPF-*Gan* tumors was confirmed by real-time RT-PCR (Figure 5*B*). When RAW264 macrophages were stimulated with LPS, expression of COX-2 and mPGES-1, as well as proinflammatory cytokines, was elevated (Figure 5*C*). Importantly, treatment of LPS-stimulated macrophages with an EP4 inhibitor or celecoxib suppressed the induction of COX-2, IL-1β, and IL-6. Moreover, inhibition of EP4 suppressed proliferation of the primary cultured gastric epithelial cells in matrigel (Figure 5*D*). These results suggest that EP4 signaling is also important for macrophage activation and epithelial cell proliferation.

Wnt Promotion by Bacterial Infection and TNF-α Stimulation

Expression of Wnt-target genes, CD44 and Eph receptor B3 (EphB3), was significantly down-regulated in the GF-*Gan* and EP4i-*Gan* mouse stomachs (Figure 6*A*). In the wild-type mouse stomach, expression of CD44 was found only in the neck of the gastric gland, whereas EphB3 was not detected (Figure 6*B*). Notably, expression of CD44 and EphB3 was significantly induced in tumor epithelial cells of SPF-*Gan* mice, which was suppressed in GF-*Gan* mice. Consistently, the active β-catenin level was decreased in the GF-*K19-Wnt1* stomach and GF-*Gan* mouse gastric tumors compared with SPF mice (Figure 6*C*), indicating that Wnt signaling activity is suppressed under GF conditions. We previously showed that macrophage-derived TNF-α promotes Wnt signaling in gastric

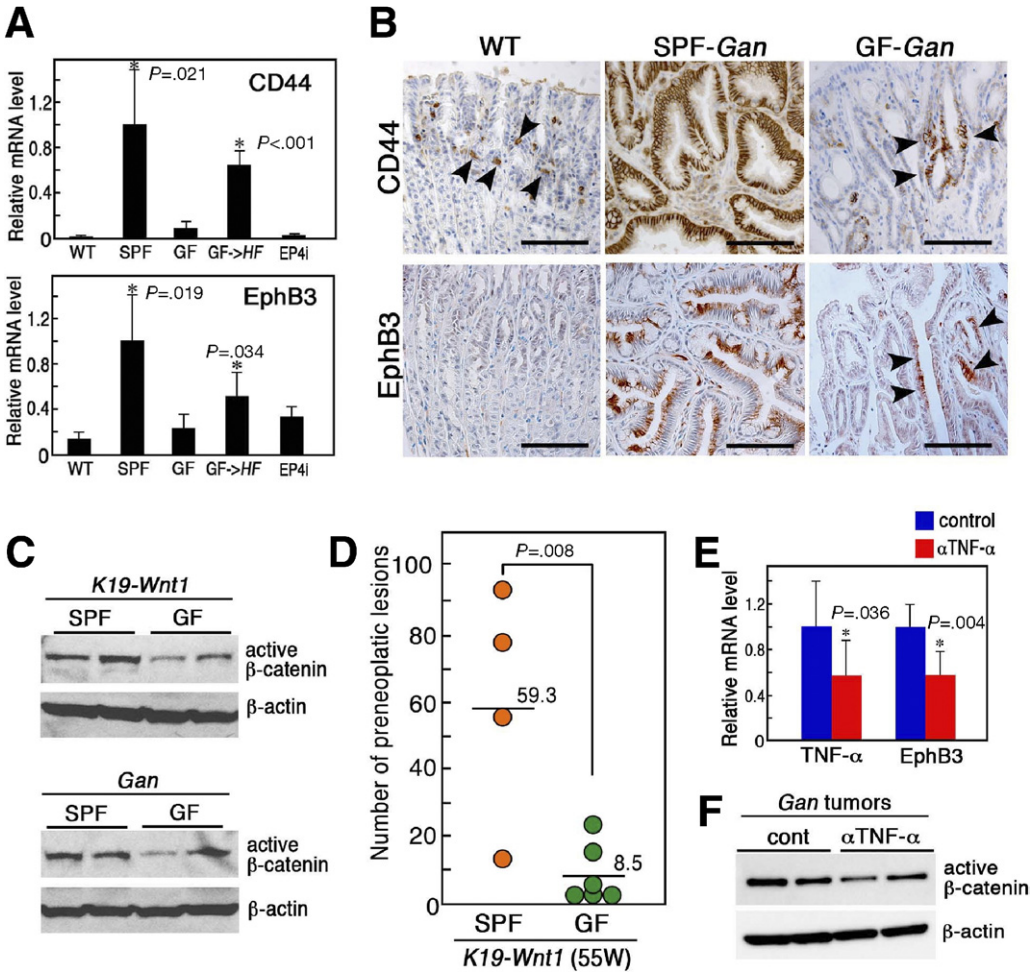

Figure 6. Wnt promotion by bacterial infection and TNF-α. (*A*) Relative messenger RNA (mRNA) levels of Wnt-target genes, CD44 and EphB3, in the wild-type mouse stomach (*WT*) and SPF-*Gan* (*SPF*), GF-*Gan* (*GF*), *H felis*-infected GF-*Gan* (*GF->HF*), and EP4 inhibitor-treated-*Gan* (*EP4i*) mouse gastric tumors (mean ± standard deviation [SD]). *$P < .05$ vs wild-type level. (*B*) Immunostaining of CD44 (*top*) and EphB3 (*bottom*) in the wild-type mouse stomach (*left*) and SPF-*Gan* (*center*) and GF-*Gan* (*right*) mouse tumors. *Arrowheads* indicate immunostained epithelial cells in the wild-type (*WT*) and GF-*Gan* mice. *Scale bars*, 100 μm. (*C*) Immunoblotting of active β-catenin in the SPF-*K19-Wnt1* and GF-*K19-Wnt1* mouse stomach (*top*) and SPF-*Gan* and GF-*Gan* mouse gastric tumors (*bottom*). β-Actin was used as an internal control. (*D*) The number of preneoplastic lesions developed in SPF-*K19-Wnt1* (*SPF*) and GF-*K19-Wnt1* (*GF*) mice. The mean numbers are indicated. (*E*) The mRNA levels of TNF-α and EphB3 in the gastric tumors of the anti-TNF-α neutralizing antibody-treated *Gan* (*αTNF-α*) relative to those of untreated control *Gan* mice (control) (mean ± SD). *$P < .05$ vs control. (*F*) Immunoblotting of active β-catenin in control (*cont*) and anti-TNF-α antibody-treated (*αTNF-α*) *Gan* mouse tumors.

cancer cells.[25] It is therefore possible that the decreased level of TNF-α in the GF-*Gan* and EP4i-*Gan* mouse stomachs resulted in suppression of Wnt signaling.

K19-Wnt1 mice develop preneoplastic lesions caused by promotion of Wnt signaling by macrophage-derived TNF-α[25] (Supplementary Table 1). Importantly, the number of preneoplastic lesions decreased significantly in the GF-*K19-Wnt1* mice compared with the SPF-*K19-Wnt1* mice (Figure 6*D*), suggesting that bacterial colonization is important for macrophage recruitment, which triggers TNF-α-induced Wnt promotion.

We next investigated whether TNF-α promotes Wnt signaling in the gastric tumor tissues. Treatment of the SPF-*Gan* mice with an anti-TNF-α neutralizing antibody resulted in down-regulation of TNF-α in tumors, possibly caused by suppression of macrophage activation (Figure 6*E*). Importantly, expression of EphB3, a Wnt-target gene, was also down-regulated. Consistently, the active β-catenin level decreased in gastric tumors by TNF-α inhibition (Figure 6*F*). These results indicate that macrophage-derived TNF-α enhances Wnt activity in gastric tumors, which may promote gastric tumorigenesis.

Discussion

Accumulating evidence has indicated that infection-associated inflammation plays an important role in cancer development.[2] Bacterial infection stimulates toll-like receptors, which induces activation of the nuclear factor-κB (NF-κB) pathway. The activation of NF-κB causes tumor promotion through induction of growth factors and suppression of apoptosis.[26] NF-κB activation

also induces COX-2 expression, which is followed by induction of the PGE_2 pathway. The COX-2/PGE_2 pathway plays a key role in intestinal tumorigenesis.[8,9] These results indicate that infection plays a key role in the activation of the NF-κB and PGE_2 pathways, which promotes tumorigenesis. In the present study, we infected *H felis* at 30 weeks of age to examine the effect of infection in tumorigenesis because we found a significant suppression of tumorigenesis in GF-*Gan* stomach at 30 weeks of age. Importantly, *H felis* infection in GF-*Gan* mice induced gastric tumor development by 55 weeks. Accordingly, the present study indicates that bacterial infection is still required for tumorigenesis even after the induction of the PGE_2 pathway.

It has been shown that PGE_2 signaling through EP4 receptor is important for intestinal tumorigenesis through the activation of epidermal growth factor receptor.[10] The current results also showed EP4 to play an important role in tumorigenesis. Bacterial colonization and EP4 signaling cooperatively induce expression of macrophage-tropic chemokine CCL2. It has been shown that CCL2 signaling is important for macrophage infiltration in colon cancers in the intestinal tumorigenesis.[22] Accordingly, it is possible that expression of CCL2 induced by bacterial colonization and EP4 signaling is important for macrophage recruitment in gastric tumorigenesis.

Intestinal commensal bacteria stimulate the toll-like receptors in the mucosa, which is important for the proliferation of undifferentiated epithelial cells.[16] Moreover, macrophages are an important niche component for the proliferation of intestinal progenitor cells in the tissue repair process.[27] Accordingly, it is possible that the innate immune response to commensal bacteria is important for the proliferation of tumor epithelial cells through macrophage recruitment. On the other hand, acquired immunity by T cells is essential for *H felis*-associated gastric pathology.[28] It is thus possible that T cells play a role in gastric tumorigenesis in *H felis*-infected GF-*Gan* mice. However, hyperplasia still developed, and the macrophages were polarized to M2, in the SPF-*Rag2*$^{-/-}$ *K19-C2mE* mouse stomach[29] (Supplementary Figure 5*D*), suggesting that increased PGE_2 levels and commensal flora can trigger these gastric phenotypes without T-cell response.

We previously showed that macrophage-derived TNF-α promotes Wnt signaling activity in gastric cancer cells, which contributes to gastric tumorigenesis.[25] Moreover, Wnt activation levels correlate with the incidence of intestinal tumorigenesis in *Apc* knockout mice,[30] and promotion of Wnt signaling activity may play an important role in malignant progression.[31] In the present study, inhibition of TNF-α resulted in a decrease in Wnt signaling activity in gastric tumors, confirming that TNF-α functions as a Wnt promoting factor in vivo. Notably, Wnt activity in the gastric tumors of GF-*Gan* mice was lower than that of SPF-*Gan* mice, which may have been caused by a decreased level of macrophage-derived TNF-α. Accordingly, it is possible that TNF-α-dependent Wnt promotion is one of the important mechanisms by which macrophages induce tumorigenesis, which is triggered by bacterial colonization and EP4 signaling.

The COX-2/PGE_2 pathway has been shown to suppress the T helper 1 immune response in the *H pylori*-infected stomach.[32] Notably, nonsteroidal anti-inflammatory drug treatment suppresses gastric carcinogenesis in the insulin-gastrin transgenic (INS-GAS) gastric tumor model mice. However, nonsteroidal anti-inflammatory drug treatment enhances gastritis in *Helicobacter*-infected INS-GAS mice, which may promote gastric tumorigenesis.[17] These results suggest that the PGE_2 pathway suppresses infection-associated carcinogenesis, which appears to be inconsistent with the present results. However, the present results indicate that commensal flora with low bacterial counts can elicit gastritis when the mucosal PGE_2 level is increased, and such commensal flora and PGE_2-dependent inflammation are important for gastric tumorigenesis. It is therefore possible that the role of PGE_2 for immune responses and tumorigenesis varies according to the level of infection status, such as exogenous aggressive infection by *Helicobacter* or commensal colonization, although this remains to be investigated.

In conclusion, bacterial infection or colonization, in cooperation with PGE_2 signaling through the EP4 receptor, induces expression of CCL2, resulting in macrophage recruitment to gastric mucosa. TNF-α produced by macrophages promotes Wnt signaling in the tumor cells, which may promote gastric tumorigenesis. Accordingly, the eradication and inhibition of the PGE_2 pathway may be an effective strategy for preventing gastric cancer development.

Supplementary Material

Note: To access the supplementary material accompanying this article, visit the online version of *Gastroenterology* at www.gastrojournal.org, and at doi: 10.1053/j.gastro.2010

References

1. Correa P, Camargo MC, Piazuelo MB. Overview and pathology of gastric cancer. In: Wang TC, Fox JG, Giraud AS, eds. The biology of gastric cancer. New York: Springer, 2008:1–24.
2. Coussens LM, Werb Z. Inflammation and cancer. Nature 2002; 420:860–867.
3. Balkwill F, Mantovani A. Inflammation and cancer: back to Virchow. Lancet 2001;357:539–545.
4. Mantovani A, Allavena P, Sica A, et al. Cancer-related inflammation. Nature 2008;454:436–444.
5. El-Omar EM, Carrington M, Chow WH, et al. Interleukin-1 polymorphisms associated with increased risk of gastric cancer. Nature 2000;404:398–402.

6. Oshima M, Dinchuk JE, Kargman SL, et al. Suppression of intestinal polyposis in *Apc*$^{\Delta 716}$ knockout mice by inhibition of cyclooxygenase 2 (COX-2). Cell 1996;87:803–809.
7. Gupta RA, DuBois RN. Colorectal cancer prevention and treatment by inhibition of cyclooxygenase-2. Nat Rev Cancer 2001;1:11–21.
8. Sonoshita M, Takaku K, Sasaki N, et al. Acceleration of intestinal polyposis through prostaglandin receptor EP2 in *Apc*$^{\Delta 716}$ knockout mice. Nat Med 2001;7:1048–1051.
9. Wang D, Wang H, Shi Q, et al. Prostaglandin E_2 promotes colorectal adenoma growth via transactivation of the nuclear peroxisome proliferators-activated receptor δ. Cancer Cell 2004;6:285–295.
10. Buchanan F, Gorden DL, Matta P, et al. Role of β-arrestin 1 in the metastatic progression of colorectal cancer. Proc Natl Acad Sci U S A 2006;103:1492–1497.
11. Saukkonen K, Rintahaka J, Sivula A, et al. Cyclooxygenase-2 and gastric carcinogenesis. APMIS 2003;111:915–925.
12. Sun WH, Yu Q, Shen H, et al. Roles of *Helicobacter pylori* infection and cyclooxygenase-2 expression in gastric carcinogenesis. World J Gastroenterology 2004;10:2809–2813.
13. Oshima H, Oshima M, Inaba T, et al. Hyperplastic gastric tumors induced by activated macrophages in COX-2/mPGES-1 transgenic mice. EMBO J 2004;23:1669–1678.
14. Qian BZ, Pollard JW. Macrophage diversity enhances tumor progression and metastasis. Cell 2010;141:39–51.
15. Oshima H, Matsunaga A, Fujimura T, et al. Carcinogenesis in mouse stomach by simultaneous activation of the Wnt signaling and prostaglandin E_2 pathway. Gastroenterology 2006;131:1086–1095.
16. Rakoff-Nahoum S, Paglino J, Eslami-Varzaneh F, et al. Recognition of commensal microflora by Toll-like receptors is required for intestinal homeostasis. Cell 2004;118:229–241.
17. Lee CW, Rickman B, Rogers AB, et al. Combination of sulindac and antimicrobial eradication of *Helicobacter pylori* prevents progression of gastric cancer in hypergastrinemic INS-GAS mice. Cancer Res 2009;69:8166–8174.
18. Takeuchi K, Tanaka A, Kato S, et al. Effect of (S)-4-(1-(5-Chloro-2-(4-fluorophenyoxy)benzamido)ethyl) benzoic acid (CJ-42794), a selective antagonist of prostaglandin E receptor subtype 4, on ulcerogenic and healing responses in rat gastrointestinal mucosa. J Pharmacol Exp Ther 2007;322:903–912.
19. Kaparakis M, Walduck AK, Price JD, et al. Macrophages are mediators of gastritis in acute *Helicobacter pylori* infection in C57BL/6 mice. Infect Immun 2008;76:2235–2239.
20. van Rooijen N, Sanders A. Liposome mediated depletion of macrophages: mechanism of action, preparation of liposomes and applications. J Immunol Methods 1994;174:83–93.
21. Oshima H, Itadani H, Kotani H, et al. Induction of prostaglandin E_2 pathway promotes gastric hamartoma development with suppression of bone morphogenetic protein signaling. Cancer Res 2009;69:2729–2733.
22. Popivanova BK, Kostadinova FI, Furuichi K, et al. Blockade of a chemokine, CCL2, reduces chronic colitis-associated carcinogenesis in mice. Cancer Res 2009;69:7884–7892.
23. Mantovani A, Sozzani S, Locati M, et al. Macrophage polarization: tumor-associated macrophages as a paradigm for polarized M2 mononuclear phagocytes. TRENDS Immunol 2002;23:549–555.
24. DeNardo DG, Barreto JB, Andreu P, et al. CD4$^+$ T cell regulates pulmonary metastasis of mammary carcinomas by enhancing protumor properties of macrophages. Cancer Cell 2009;16:91–102.
25. Oguma K, Oshima H, Aoki M, et al. Activated macrophages promote Wnt signaling through tumour necrosis factor-α in gastric tumour cells.EMBO J 2008;27:1671–1681.
26. Greten FR, Eckmann, L, Greten TF, et al. IKKβ links inflammation and tumorigenesis in a mouse model of colitis-associated cancer. Cell 2004;118:285–296.
27. Pull SL, Doherty JM, Mills JC, et al. Activated macrophages are an adaptive element of the colonic epithelial progenitor niche necessary for regenerative responses to injury. Proc Natl Acad Sci U S A 2005;102:99–104.
28. Roth KA, Kapadia SB, Martin SM, et al. Cellular immune responses are essential for the development of *Helicobacter felis*-associated gastric pathology. J Immunol 1999;163:1490–1497.
29. Oshima M, Oshima H, Matsunaga A, et al. Hyperplastic gastric tumors with spasmolytic polypeptide-expressing metaplasia caused by tumor necrosis factor-α-dependent inflammation in cyclooxygenase-2/microsomal prostaglandin E sunthase-1 transgenic mice. Cancer Res 2005;65:9147–9151.
30. Li Q, Ishikawa TO, Oshima M, et al. The threshold level of adenomatous polyposis coli protein for mouse intestinal tumorigenesis. Cancer Res 2005;65:8622–8627.
31. Fodde R, Brabletz T. Wnt/β-catenin signaling in cancer stemness and malignant behavior. Curr Opin Cell Biol 2007;19,150–158.
32. Meyer F, Ramanujam KS, Gobert AP, et al. Cutting edge: cyclooxygenase-2 activation suppresses Th1 polarization in response to *Helicobacter pylori*. J Immunol 2003;171:3913–3917.

Received December 3, 2009. Accepted November 3, 2010.

Reprint requests

Address requests for reprints to: Masanobu Oshima, DVM, PhD, Division of Genetics, Cancer Research Institute, Kanazawa University, Kakuma-machi, Kanazawa, 920-1192 Japan. e-mail: oshimam@kenroku.kanazawa-u.ac.jp;fax: (81) 76-234-4519.

Acknowledgments

The authors thank Manami Watanabe for her excellent technical assistance.

K.O. is a Research Fellow of the Japan Society for the Promotion of Science, Japan.

Conflicts of interest

The authors disclose no conflicts.

Funding

Supported by Grants-in-Aid from the Ministry of Education, Culture, Sports, Science and Technology of Japan and the Ministry of Health, Labour and Welfare of Japan.

Supplementary Materials and Methods

Depletion of Indigenous Bacteria

To deplete indigenous bacteria in the stomach, specific pathogen free (SPF)-*Gan* (*Gan* for Gastric neoplasia) mice (n = 5) were administered ampicillin (1 g/L; Sigma, St. Louis, MO), vancomycin (500 mg/L; Sigma), neomycin sulfate (1 g/L; Sigma), and metronidazole (1g/L; Sigma) in drinking water as previously described.[1] Gastric tumors were examined by x-ray computerized tomography using a LaTheta LCT-100 instrument (Aloka, Tokyo, Japan) after 0, 2, and 4 weeks of antibiotic administration. The mean tumor area was calculated from computerized tomography images using a National Institute of Health (NIH) Image J software program (Bethesda, MD).

Histology and Immunohistochemistry

Stomach tissue specimens were fixed in 4% paraformaldehyde, paraffin-embedded, and sectioned at 4-μm thickness. Frozen sections were used for CD4 immunostaining. The construction of SPF-*Rag2*$^{-/-}$*K19-C2mE* mice was described previously.[2] Antibodies for β-catenin (Sigma), mannose receptor (AbD Serotec, Raleigh, NC), CD3ε (Santa Cruz Biotechnology, Santa Cruz, CA), and CD4 (BD Pharmingen, Columbus, NE) were used as the primary antibodies. Alexa Fluor 594 or Alexa Fluor 488 antibody (Molecular Probes, Eugene, OR) was used as the secondary antibody. Infection of *Helicobacter felis* in the gastric glands was confirmed using hematoxyin-stained paraffin sections of the *H felis*-infected germfree-*Gan* mouse stomach at $\times$1000 magnification.

Expression Analysis of M2 Macrophage Markers

The expression profiles of M2 macrophage markers Ym1, Ym2, arginase 1 (Arg1), and transforming growth factor-β1 in *Gan*, *K19-C2mE*, and wild-type mouse stomachs were downloaded from the National Center for Biotechnology Information Gene Expression Omnibus (GEO; accession number GSE16902). These expression data were transformed to log10 ratios to the average of wild-type mouse samples.

References

1. Rakoff-Nahoum S, Paglino J, Eslami-Varzaneh F, et al. Recognition of commensal microflora by Toll-like receptors is required for intestinal homeostasis. Cell 2004;118:229–241.
2. Oshima M, Oshima H, Matsunaga A, et al. Hyperplastic gastric tumors with spasmolytic polypeptide-expressing metaplasia caused by tumor necrosis factor-α-dependent inflammation in cyclooxygenase-2/microsomal prostaglandin E sunthase-1 transgenic mice. Cancer Res 2005;65:9147–9151.
3. Oshima H, Matsunaga A, Fujimura T, et al. Carcinogenesis in mouse stomach by simultaneous activation of the Wnt signaling and prostaglandin E_2 pathway. Gastroenterology 2006;131:1086–1095.
4. Oshima H, Oshima M, Inaba T, et al. Hyperplastic gastric tumors induced by activated macrophages in COX-2/mPGES-1 transgenic mice. EMBO J 2004;23:1669–1678.

Supplementary Table 1. Genotypes and Phenotypes of Transgenic Mouse Models

Strain name	Transgene(s)	Phenotypes in the glandular stomach (reference)
K19-Wnt1	*Wnt1*	Activation of canonical Wnt signaling Small preneoplastic lesions consisting of Wnt-promoted epithelial cells with macrophage infiltration and activation.[3]
K19-C2mE	*Ptgs2* and *Ptges*, encoding COX-2 and mPGES-1, respectively	Activation of PGE$_2$ pathway Hyperplasia consisting of TFF2-positive metaplastic mucous cells associated with inflammatory infiltration.[2,4]
K19-Wnt1/C2mE (*Gan* for Gastric neoplasia)	*Wnt1*, *Ptgs2*, and *Ptges*	Activation of both Wnt and PGE$_2$ pathways Development of dysplastic tumors with the infiltration of macrophages.[3]

PGE$_2$, prostaglandin E$_2$; COX-2, cyclooxygenase-2; *Ptgs2*, gene symbol for mouse COX-2; mPGES-1, microsomal prostaglandin E synthase-1; *Ptges*, gene symbol for mouse mPGES-1; TFF2, trefoil factor 2.

Supplementary Table 2. Results of Germfree Monitoring Tests

Samples	Feces			Bedding			Swab	
Media	TGC[a]		PDB[b]	TGC		PDB	PDB	
Temp[c]	37	RT	RT	37	RT	RT	RT	Fecal smear
Mouse age, wks								
2	—	—	—	—	—	—	—	—
3	—	—	—	—	—	—	—	—
5	—	—	—	—	—	—	—	—
10	—	—	—	—	—	—	—	—
15	—	—	—	—	—	—	—	—
20	—	—	—	—	—	—	—	—
23	—	—	—	—	—	—	—	—
28	—	—	—	—	—	—	—	—
31	—	—	—	—	—	—	—	—
45	—	—	—	—	—	—	—	—
50	—	—	—	—	—	—	—	—
55	—	—	—	—	—	—	—	—

RT, room temperature; Temp, temperature.
[a]Thioglycollate medium.
[b]Potato dextrose broth.
[c]Samples were incubated in TGC at 37°C or at room temperature or in PDB at room temperature.

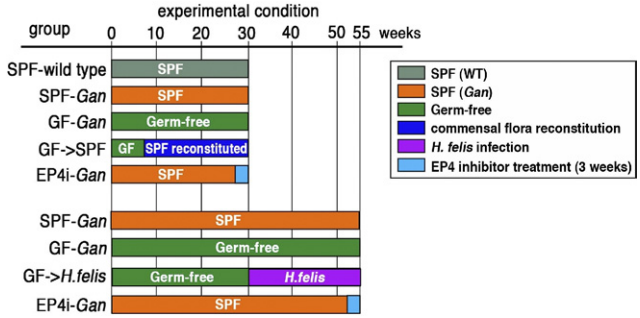

Supplementary Figure 1. A schematic illustration of the experimental schedule. The gastric phenotypes of specific pathogen free (SPF)-*Gan* and germfree (GF)-*Gan* mice were examined at 30 and 55 weeks of age. GF-*Gan* mice were reconstituted with commensal flora at 7 weeks of age, and gastric phenotypes were examined at 30 weeks of age. The EP4 inhibitor was administered for 3 weeks from 27 or 52 weeks of age. GF-*Gan* mice were infected with *Helicobacter felis* at 30 weeks of age, and infected mice were examined at 55 weeks of age.

Supplementary Table 3. List of Excluded Pathogens in Animal Room 4 of SPF Facility, Kanazawa University

Bordetella bronchiseptica
Citrobacter rodentium
Corynebacterium kutscheri
Mycoplasma pulmonis
Pasteurella pneumotropica
Salmonella spp
Streptococcus pneumoniae
Pseudomonas aeruginosa
Helicobacter hepaticus
Clostridium piliforme
Ectromelia virus
Sialodacryoadenitis virus (SDAV)
Hanta virus
Lymphocytic choriomeningitis virus (LCMV)
Mouse hepatitis virus
Sendai virus
Intestinal protozoas (*Giardia muris*, *Spironucleus muris*, *Tritrichomonas muris*, *Octomitus pulcher*, Coccidiosis)
Helminths (*Aspiculuris tetraptera*, *Syphacia obvelata*)
Parasites (*Myobia* sp, *Polyplaxserrata*)

NOTE. All SPF mice used in the present study were raised in this SPF room.
SPF, specific antigen free.

Supplementary Table 4. Primer Sequences for Real-time RT-PCR

Gene name	Forward primer	Reverse primer
COX-2	GTGTGCGACATACTCAAGCAGGA	TGAAGTGGTAACCGCTCAGGTG
mPGES-1	CTGCAGCACACTGCTGGTCA	CTCCACATCTGGGTCACTCCTGTA
TNF-α	AAGCCTGTAGCCCACGTCGTA	GGCACCACTAGTTGGTTGTCTTTG
IL-1β	TCCAGGATGAGGACATGAGCAC	GAACGTCACACACCAGCAGGTTA
IL-6	CCACTTCACAAGTCGGAGGCTTA	GCAAGTGCATCATCGTTGTTCATAC
KC(CXCL1)	GCTTGAAGGTGTTGCCCTCAG	AAGCCTCGCGACCATTCTTG
MIP-2(CXCL2)	GCGCTGTCAATGCCTGAAGA	TTTGACCGCCCTTGAGAGTG
CCL2	GCATCCACGTGTTGGCTCA	CTCCAGCCTACTCATTGGGATCA
CCL3	TGAAACCAGCAGCCTTTGCTC	AGGCATTCAGTTCCAGGTCAGTG
CCL4	CCATGAAGCTCTGCGTGTCTG	GGCTTGGAGCAAAGACTGCTG
CCL5	ACCAGCAGCAAGTGCTCCAA	TGGCTAGGACTAGAGCAAGCAATG
CCL7	GCATCCACATGCTGCTATGTCA	GATGGGCTTCAGCACAGACTTC
CCL8	TGCCTGCTGCTCATAGCTGTC	GACATACCCTGCTTGGTCTGGAA
EP4	GTGGTGCTCATCTGCTCCATTC	CTGCAAATCTGGGTTTCTGCTG
CD44	TTTAACCTATATGCAGCAAGCCACT	CAGAATCATCACCACTATGGCAAG
EphB3	AGCTGTGAATATCACCACCAACCA	TGACTCCATTAGGCCGCTCTG

COX-2, cyclooxygenase-2; IL-1β, interleukin-1β; IL-6, interleukin-6; mPGES-1, microsomal prostaglandin E synthase-1; RT-PCR, reverse-transcription polymerase chain reaction; TNF-α, tumor necrosis factor-α; KC, keratinocyte-derived chemokine; MIP-2, macrophage inflammatory protein-2; CXCL, chemokine (C-X-C motif) ligand; CCL, chemokine (C-C motif) ligand; EP4, PGE_2 receptor subtype 4; EphB3, Eph receptor B3.

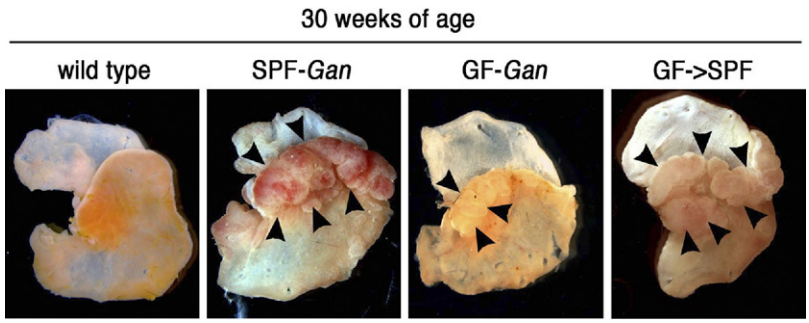

Supplementary Figure 2. Representative photographs of gastric tumor phenotypes at 30 weeks of age. Wild-type mouse stomach, gastric tumors of SPF-*Gan* mouse, GF-*Gan* mouse, and GF-*Gan* mouse reconstituted with commensal bacteria (GF->SPF) are shown (from left to right). *Arrowheads* indicate gastric tumors in SPF-*Gan*, GF-*Gan*, and GF->SPF *Gan* mice.

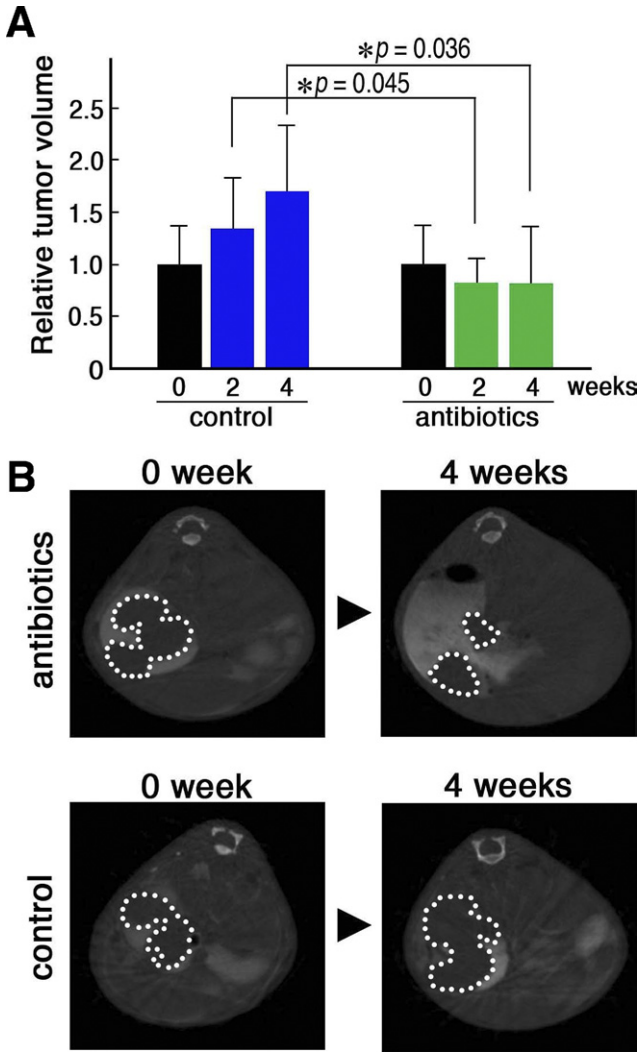

Supplementary Figure 3. Suppression of gastric tumor growth by antibiotic treatment. (*A*) The mean tumor volumes calculated from x-ray computerized tomography (CT) images of control *Gan* mice (*blue bars*, *left*) and antibiotics-treated *Gan* mice (*green bars*, *right*) relative to the level at 0 weeks of treatment (*closed bars*) (mean ± standard deviation). *$P < .05$. (*B*) Representative x-ray CT images of gastric tumors of the same mice from the antibiotics-treated group (*top*) and control group (*bottom*) at 0 and 4 weeks of antibiotic treatment. The *dashed lines* indicate gastric tumors. Note that tumor growth was suppressed by treatment with antibiotics (*top*).

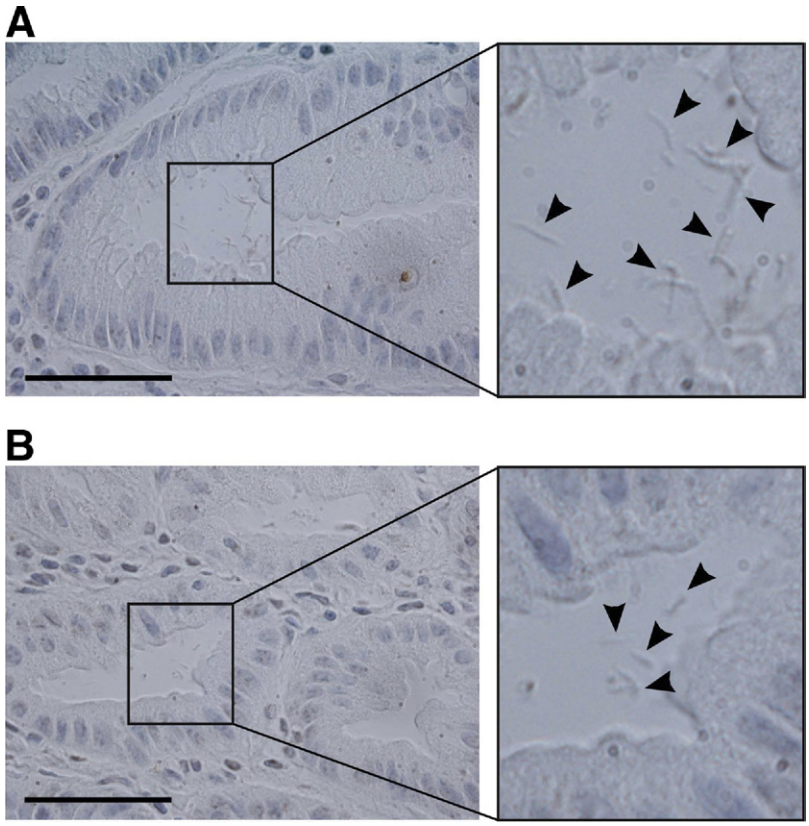

Supplementary Figure 4. Infection of *Helicobacter felis* in the lumen of the *H felis*-infected GF-*Gan* mouse gastric glands (*A* and *B*). *Arrowheads* indicate *H felis*. *Scale bars*, 50 μm. Original magnification, ×1000.

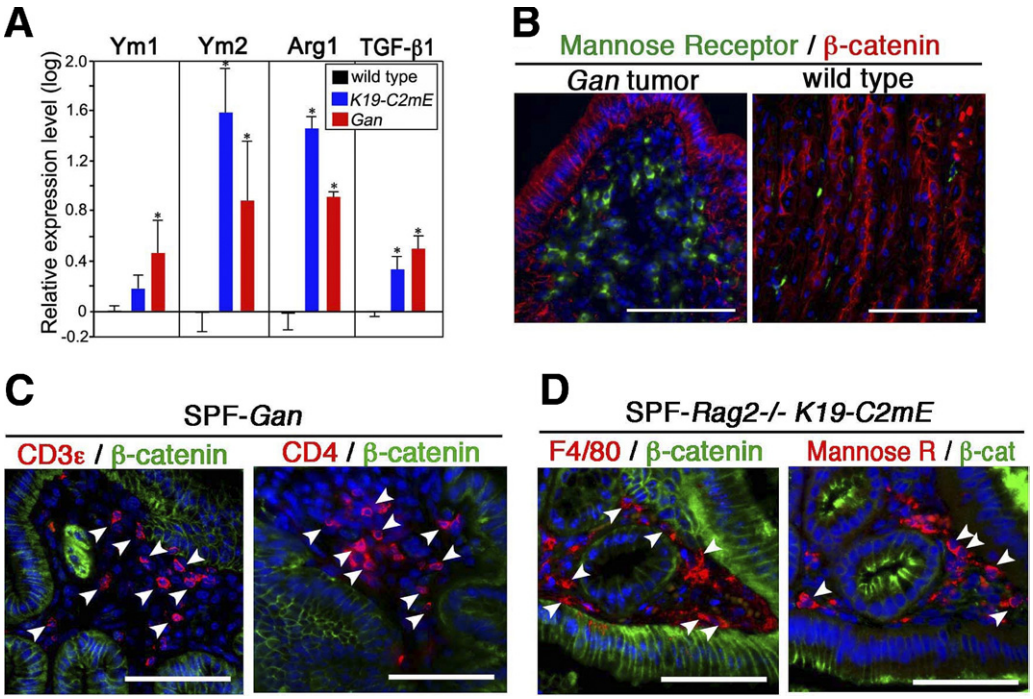

Supplementary Figure 5. M2 macrophages in *Gan* and *K19-C2mE* mouse stomachs. (*A*) The relative expression level of M2 macrophage markers—Ym1, Ym2, arginase 1 (Arg1), and transforming growth factor (TGF)-β1—in the *K19-C2mE* mouse stomach (*blue*) and *Gan* mouse tumors (*red*) in comparison with that in the wild-type mouse stomach (*black*) (mean log10 ratio with standard deviation). *$P < .05$ vs wild-type level. (*B*) Immunostaining of M2 macrophage marker, mannose receptor (*green*) and β-catenin (*red*) with 4',6-diamidino-2-phenylindole (DAPI) nuclear staining (*blue*) in *Gan* mouse tumors (*left*) and wild-type mouse stomach (*right*). (*C*) Immunostaining of CD3ε (*left*, *red*, *arrowheads*) or CD4 (*right, red*, *arrowheads*) and β-catenin (*green*) with DAPI staining (*blue*) of SPF-*Gan* mouse tumors. (*D*) Immunostaining of F4/80 (*left*, *red*, *arrowheads*) or mannose receptor (*right, red*, *arrowheads*) and β-catenin (*green*) with DAPI staining (*blue*) of the SPF-*Rag2*$^{-/-}$ *K19-C2mE* mouse stomach. Note that mannose receptor-expressing M2 macrophages were found in the T cell-depleted Rag2$^{-/-}$ *K19-C2mE* mouse inflamed stomach. *Scale bars* in *B–D*, 100 μm.